

Sum rules and energy scales in the high-temperature superconductor $\text{YBa}_2\text{Cu}_3\text{O}_{6+x}$

C. C. Homes* and S. V. Dordevic

Department of Physics, Brookhaven National Laboratory, Upton, New York 11973, USA

D. A. Bonn, Ruixing Liang, and W. N. Hardy

Department of Physics and Astronomy, University of British Columbia, Vancouver, British Columbia, Canada V6T 1Z1

(Received 19 March 2003; revised manuscript received 1 August 2003; published 22 January 2004)

The Ferrell-Glover-Tinkham (FGT) sum rule has been applied to the temperature dependence of the in-plane optical conductivity of optimally doped $\text{YBa}_2\text{Cu}_3\text{O}_{6.95}$ and underdoped $\text{YBa}_2\text{Cu}_3\text{O}_{6.60}$. Within the accuracy of the experiment, the sum rule is obeyed in both materials. However, the energy scale ω_c required to recover the full strength of the superfluid ρ_s in the two materials is dramatically different; $\omega_c \approx 800 \text{ cm}^{-1}$ in the optimally doped system (close to twice the maximum of the superconducting gap $2\Delta_0$), but $\omega_c \gtrsim 5000 \text{ cm}^{-1}$ in the underdoped system. In both materials, the normal-state scattering rate close to the critical temperature is small, $\Gamma < 2\Delta_0$, so that the materials are not in the dirty limit and the relevant energy scale for ρ_s in a BCS material should be twice the energy gap. The FGT sum rule in the optimally doped material suggests that the majority of the spectral weight of the condensate comes from energies below $2\Delta_0$, which is consistent with a BCS material in which the condensate originates from a Fermi-liquid normal state. In the underdoped material the larger energy scale may be a result of the non-Fermi-liquid nature of the normal state. The dramatically different energy scales suggest that the nature of the normal state creates specific conditions for observing the different aspects of what is presumably a central mechanism for superconductivity in these materials.

DOI: 10.1103/PhysRevB.69.024514

PACS number(s): 74.25.Gz, 78.30.-j

I. INTRODUCTION

Sum rules and conservation laws play an important role in physics. In spectroscopy, the conductivity sum rule is particularly useful and is an expression of the conservation of charge.¹ In metallic systems, the conductivity sum rule usually yields the classical plasma frequency or the effective number of carriers. In superconductors, below the critical temperature T_c some fraction of the carriers collapse into the $\delta(\omega)$ function at zero frequency that determines the London penetration depth λ_L , with a commensurate loss of spectral weight from low frequencies (below twice the superconducting energy gap 2Δ). This shift in spectral weight may be quantified by the application of the conductivity sum rule to the normal and superconducting states, as discussed by Ferrell, Glover, and Tinkham (the FGT sum rule),^{2,3} which is used to estimate the strength of the superconducting condensate $\rho_s = c^2/\lambda_L^2$. The theory of superconductivity described by Bardeen, Cooper, and Schrieffer (BCS) holds that while the kinetic energy of the superconducting state is greater than that of the normal state,^{4,5} this increase is compensated by the reduction in potential energy which drives the transition (the net reduction of energy is simply the condensation energy). However, it has been proposed that in certain hole-doped materials the superconductivity could arise from a lowering of the kinetic rather than the potential energy.⁶ In such a system nonlocal transfers of spectral weight result in the apparent violation of the FGT sum rule, and yield a value for the strength of ρ_s that would be too small (λ_L would be too large).⁶⁻⁸ Similar models in the cuprate materials presume either strong coupling,^{9,10} or that the normal state is not a Fermi liquid and that superconductivity is driven either by the recovery of frustrated kinetic energy when pairs are formed,^{11,12} by lowering the in-plane zero-point kinetic

energy,¹³ or by the condensation of preformed pairs.¹⁴

Experimental results along the poorly conducting inter-plane (c -axis) direction in several different cuprate materials support the view that the kinetic energy is reduced below the superconducting transition.¹⁵⁻¹⁷ In some materials, the low-frequency c -axis spectral weight accounts for only half of the strength of the condensate. However, this violation of the FGT sum rule appears to be restricted to the underdoped materials which display a pseudogap in the conductivity.¹⁸ The dramatically lower value of the strength of the condensate along the c axis makes it easier to observe kinetic energy contributions. In comparison, the much larger value of the condensate in the copper-oxygen planes makes it much more difficult to observe changes due to the kinetic energy based on optical sum rules.^{19,20} Recently, high-precision measurements in the near-infrared and visible region have reported small changes in the in-plane spectral weight associated with the onset of superconductivity, supporting the argument that changes in the kinetic energy are indeed occurring.²¹⁻²³ While the relatively small changes of the in-plane spectral weight make it difficult to make statements about the kinetic energy, it is nonetheless a strong motivation to examine the evolution of the spectral weight in detail to see if there are unexpected signatures of an unconventional mechanism for the superconductivity in this class of materials.

In this paper we examine the changes of the in-plane spectral weight and the evolution of the superconducting condensate in the optimally doped and underdoped detwinned $\text{YBa}_2\text{Cu}_3\text{O}_{6+x}$ single crystals for light polarized perpendicular to the copper-oxygen chains, along the a axis. The BCS model requires that the spectral weight of the condensate be fully formed at energies comparable to the energy gap ($\omega_c \approx 2\Delta$), with no subsequent violation of the FGT sum

rule. This is precisely what is observed for the optimally doped material, within the limits of experimental accuracy for the sum rules, which is estimated to be about 5%. However, in the underdoped material only 80% of the spectral weight of the condensate has been recovered at energies comparable to 2Δ ; the FGT sum rule must be extended to considerably higher frequencies to recover the remaining spectral weight ($\omega_c \geq 0.6$ eV). For $T \geq T_c$, the normal-state scattering rate is determined to be small, so this shift in spectral weight cannot be attributed to dirty-limit effects in response to impurities. However, the nature of the normal state is dramatically different in the optimally doped material, which is reminiscent of a Fermi liquid, and the underdoped material, which develops a pseudogap and displays non-Fermi-liquid behavior. The dramatically different energy scales required to recover the full value of ρ_s suggest that these aspects of the superconductivity are related to the normal-state properties from which it emerges.

II. EXPERIMENT AND SAMPLE PREPARATION

Details of the growth and characterization of the mechanically detwinned $\text{YBa}_2\text{Cu}_3\text{O}_{6+x}$ crystals have been previously described in detail^{24,25} and will be discussed only briefly. The crystal had a small amount of Ni deliberately introduced, $\text{Cu}_{1-x}\text{Ni}_x$, where $x=0.0075$. Such a small concentration of Ni results in a critical temperature which is slightly lower (~ 2 K) than the pure materials, with a somewhat broader transition. The same detwinned crystal has been carefully annealed to produce two different oxygen concentrations $x=0.95$ ($T_c \approx 91$ K) and 0.60 ($T_c \approx 57$ K). The reflectance for light polarized along the a axis (perpendicular to the CuO chains, therefore probing only the CuO_2 planes) has been measured at a variety of temperatures over a wide frequency range (≈ 40 to 9000 cm^{-1}) using an over-filling technique;²⁶ this reflectance has been extended to very high frequency (3.5×10^5 cm^{-1}) using the data of Basov *et al.*^{27,28} and Romberg *et al.*²⁹ The absolute value of the reflectance is estimated to be accurate to within 0.2%. The optical properties are calculated from a Kramers-Kronig analysis of the reflectance. The optical conductivity, which dealt with the effects of Ni doping on the CuO chains and the reduction of the in-plane anisotropy, has been previously reported.³⁰ The presence of Ni in such small concentrations was not observed to have any effect on the conductivity of the CuO_2 planes in either the normal or superconducting states.

III. RESULTS AND DISCUSSION

A. Optical sum rules

Optical sum rules comprise a powerful set of tools to study and characterize the lattice vibrations and electronic properties of solids. The spectral weight may be estimated by a partial sum rule of the conductivity^{1,31}

$$N(\omega_c) = \frac{120}{\pi} \int_0^{\omega_c} \sigma_1(\omega) d\omega \xrightarrow{\omega_c \rightarrow \infty} \omega_p^2, \quad (1)$$

where $\omega_p^2 = 4\pi n e^2 / m_0$ is the classical plasma frequency, n is the carrier concentration, and m_0 is the bare optical mass. In the absence of bound excitations, this expression is exact in the limit of $\omega_c \rightarrow \infty$. However, any realistic experiment involves choosing a low-frequency cutoff ω_c . When applied to the Drude model

$$\tilde{\epsilon}(\omega) = \epsilon_\infty - \frac{\omega_p^2}{\omega(\omega + i\Gamma)}, \quad (2)$$

where ϵ_∞ is the contribution from the ionic cores, and $\Gamma = 1/\tau$ is the scattering rate, the conductivity sum rule indicates that 90% of the spectral weight is recovered for $\omega_c \sim 6\Gamma$. For even modest choices of Γ , ω_c can be quite large ($\approx \omega_p$). This places some useful constraints on the confidence limits for the conductivity sum rule in the normal state.

The conductivity in the superconducting state for any polarization \mathbf{r} has two components⁵

$$\sigma_{1,\mathbf{r}}^{\text{SC}}(\omega) = \frac{\pi}{120} \rho_{s,\mathbf{r}} \delta(\omega) + \sigma_{1,\mathbf{r}}^{\text{reg}}(\omega). \quad (3)$$

The first part is associated with the superconducting $\delta(\omega)$ function at zero frequency, where $\rho_{s,\mathbf{r}}$ is the superfluid stiffness, or strength of the superconducting order.³² This is often expressed as the square of a plasma frequency $\omega_{pS}^2 = 4\pi n_s e^2 / m_{\mathbf{r}}^*$, where n_s is the density of superconducting electrons and $m_{\mathbf{r}}^*$ is the effective mass tensor. The second component $\sigma_{1,\mathbf{r}}^{\text{reg}}(\omega)$ is referred to as the ‘‘regular’’ component for $\omega > 0$ and is associated with the unpaired charge carriers.

A variation of the conductivity sum rule in a superconductor is to study the amount of spectral weight that collapses into the superconducting $\delta(\omega)$ function at the origin below the critical temperature.⁵ This scenario is represented in Fig. 1, which shows the normalized conductivity for a BCS s -wave model for an arbitrary purity level³³ where the scattering rate in the normal state has been chosen as $\Gamma = 2\Delta$ (2Δ is the full gap value for $T \ll T_c$). The solid line shows the real part of the optical conductivity $\sigma_1(\omega)$ in the normal state for $T \geq T_c$, while the dashed line is the calculated value for $\sigma_1(\omega)$ in the superconducting state for $T \ll T_c$. For $T \ll T_c$ the gap is fully formed, and there is no conductivity for $\omega < 2\Delta$, above which the onset of absorption occurs. The missing spectral weight represented by the hatched area represents the strength of the condensate ω_{pS}^2 . This area may be estimated by the FGT sum rule^{2,3}

$$\omega_{pS}^2 = \frac{120}{\pi} \int_{0+}^{\omega_c} [\sigma_{1,n}(\omega) - \sigma_{1,s}(\omega)] d\omega, \quad (4)$$

where $\sigma_{1,n}(\omega) \equiv \sigma_1(\omega, T \geq T_c)$ and $\sigma_{1,s}(\omega) \equiv \sigma_1(\omega, T \ll T_c)$. An alternative method for extracting the superfluid density relies on only the real part of the dielectric function. Simply put, if upon entering the superconducting state for $T \ll T_c$ it is assumed that all of the carriers collapse into the condensate, then $\omega_{pS} \equiv \omega_p$ and $\Gamma \rightarrow 0$, so that the form of the dielectric function in Eq. (2) becomes $\epsilon_1(\omega) = \epsilon_\infty - \omega_p^2 / \omega^2$; in the

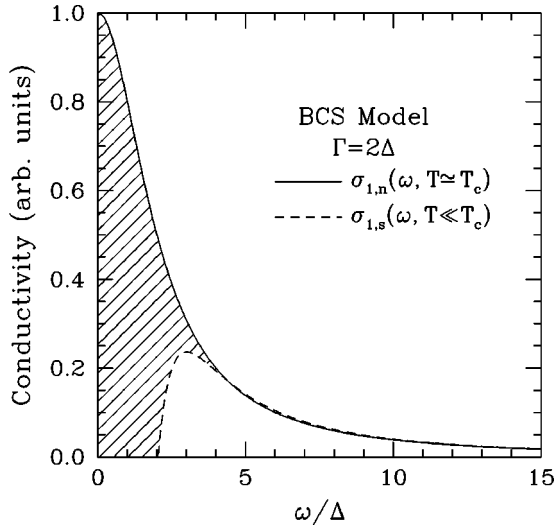


FIG. 1. The real part of the optical conductivity calculated for a BCS model for a normal-state scattering rate of $\Gamma=2\Delta$. The conductivity in the normal state $\sigma_1(\omega, T \gtrsim T_c)$ is shown by the solid line (normalized to unity), while the conductivity in the superconducting state $\sigma_1(\omega, T \ll T_c)$ is shown by the dashed line. For $T \ll T_c$ the superconducting gap 2Δ is fully formed and there is no absorption below this energy. The hatched area illustrates the spectral weight that has collapsed into the superconducting $\delta(\omega)$ function at the origin.

limit of $\omega \rightarrow 0$, $\rho_s \propto \omega_{ps}^2 = -\omega^2 \epsilon_1(\omega)$. This is a generic result in response to the formation of a $\delta(\omega)$ function and is not model dependent. The value for $-\omega^2 \epsilon_1(\omega)$ is shown in Fig. 2 for $\Gamma=2\Delta$. There is a small dip near 2Δ (which becomes somewhat washed out for $\Gamma \gg 2\Delta$), and the curve converges cleanly in the $\omega \rightarrow 0$ limit. The determination of ρ_s from $-\omega^2 \epsilon_1(\omega)$ has two main advantages: (i) it relies only on the value of $\epsilon_1(\omega)$ for $T \ll T_c$ and thus probes just the superfluid response and (ii) ρ_s is determined in a low-frequency limit,

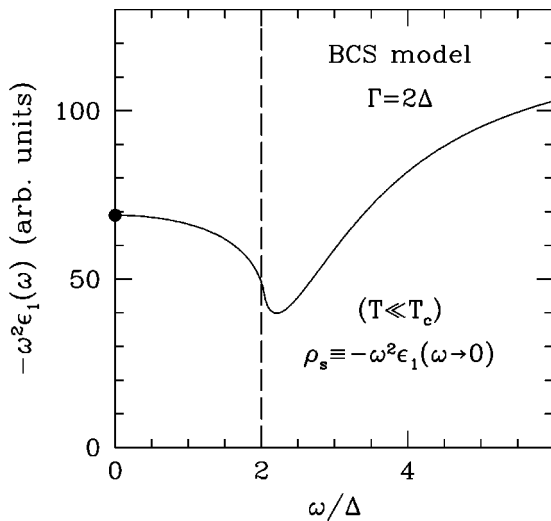


FIG. 2. The value of $-\omega^2 \epsilon_1(\omega)$ calculated from the BCS model for $T \ll T_c$ for the normal-state scattering rate $\Gamma=2\Delta$ (solid line); $\rho_s = -\omega^2 \epsilon_1(\omega)$ in the limit of $\omega \rightarrow 0$. Note that there is a slight minimum near 2Δ (long dashed line).

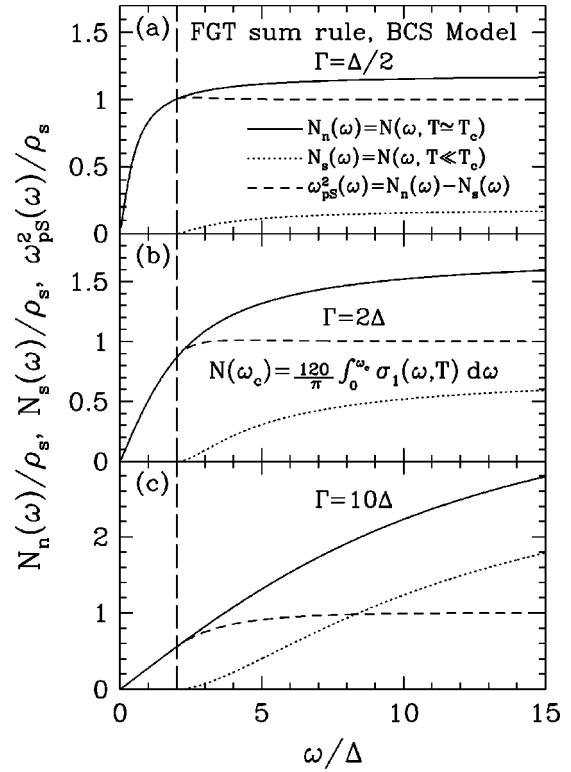


FIG. 3. The Ferrell-Glover-Tinkham (FGT) sum rule applied to a BCS model for a variety of different normal-state scattering rates. The solid line is the conductivity sum rule applied to the $\sigma_1(\omega, T \gtrsim T_c)$ [$N_n(\omega)$], while the dotted line is for $\sigma_1(\omega, T \ll T_c)$ [$N_s(\omega)$]; the dashed line is the difference between the two. The curves have been normalized to the full weight of the condensate ρ_s to yield a dimensionless ratio. (a) $\Gamma = \Delta/2$, (b) $\Gamma = 2\Delta$, and (c) $\Gamma = 10\Delta$. The spectral weight transferred from the normal state to the condensate decreases with increasing Γ , illustrating the trend from the clean- to dirty-limit case. Even for the largest value of Γ chosen, a large fraction of the condensate is captured by the integral at $\omega_c = 2\Delta$ (long-dashed line).

which removes the uncertainty of the high-frequency cutoff frequency ω_c in the FGT sum rule estimates of the condensate. We will distinguish between values of the condensate determined from $-\omega^2 \epsilon_1(\omega)$ as ρ_s , and the FGT sum rule as ω_{ps}^2 . The two techniques should in fact yield the same result, and it is indeed useful to compare the high-frequency estimates of ω_{ps}^2 with ρ_s .

The rapidity with which the spectral weight of the condensate is captured by the Ferrell-Glover-Tinkham sum rule is shown in Fig. 3 for three different choices of the normal-state scattering rate relative to the superconducting energy gap. Here the solid line is the conductivity sum rule applied to $\sigma_1(\omega)$ in the normal state ($T \gtrsim T_c$), effectively ω_p^2 , while the dotted line is the conductivity sum rule for $T \ll T_c$, which yields $\omega_p^2 - \omega_{ps}^2$. The difference between the two curves is the dashed line, which is simply ω_{ps}^2 . To simplify matters, in each case the integrals have been normalized with respect to the strength of the fully formed condensate ρ_s , to yield a dimensionless ratio. In Fig. 3(a) the normal state scattering rate has been chosen to be $\Gamma = \Delta/2$ (“clean limit”). It may be

observed that nearly all of the spectral weight in the normal state collapses into the condensate. Furthermore, the condensate is essentially fully formed above 2Δ . In Fig. 3(b) the normal-state scattering rate has been chosen to have an intermediate value $\Gamma=2\Delta$ (the situation depicted in Fig. 1). The larger value of Γ has the effect of shifting more of the normal-state spectral weight above 2Δ , which reduces the strength of the condensate. However, despite the larger value for Γ and the reduced strength of the condensate, it is once again almost fully formed by 2Δ . Finally, in Fig. 3(c) a large normal-state scattering rate $\Gamma=10\Delta$ is chosen to put the system into the dirty limit. The large scattering rate broadens the normal-state conductivity and moves a considerable amount of the spectral weight to high frequency, thus only a relatively small amount of the spectral weight is transferred to the condensate. Despite this, by 2Δ almost 60% of the condensate has been captured, and by 4Δ the condensate is almost fully formed. This demonstrates that with the exception of the dirty limit, the relevant energy scale for $\omega_c \approx 2\Delta$. This result is important to the arguments that are to follow.

B. $\text{YBa}_2\text{Cu}_3\text{O}_{6+x}$

The temperature dependence of the optical conductivity of optimally doped $\text{YBa}_2\text{Cu}_3\text{O}_{6.95}$ ($T_c \approx 91$ K) for light polarized along the a axis is shown in Fig. 4(a). The Drude-like low-frequency conductivity narrows as the temperature decreases from room temperature to just above T_c ; well below the superconducting transition the low-frequency conductivity has decreased and the missing spectral weight has collapsed into the condensate. However, an optical gap is not observed and there is a great deal of residual conductivity at low frequency. The conductivity can be reasonably well described using a “two-component” model,³⁴ with a Drude component and a number of bound excitations, usually Lorentz oscillators. While the low-frequency conductivity is satisfactorily described by a Drude term, the midinfrared region is not and a large number of oscillators are required to reproduce the conductivity. For this reason, a generalized form of the Drude model is often adopted where the scattering rate is allowed to have a frequency dependence³⁵ (in order to preserve the Kramers-Kronig relation, the effective mass must then also have a frequency dependence). The frequency-dependent scattering rate has the form³⁶

$$\frac{1}{\tau(\omega)} = \frac{\omega_p^2}{4\pi} \text{Re} \left[\frac{1}{\tilde{\sigma}(\omega)} \right]. \quad (5)$$

The value for the plasma frequency used to scale the expression in Eq. (5) has been estimated using the conductivity sum rule for $\sigma_{1,a}(\omega, T \approx T_c)$, using $\omega_c \approx 1$ eV, which yields a value for $\omega_{p,a} \approx 16700$ cm^{-1} , or about 2 eV (Ref. 30). The frequency-dependent scattering rate $1/\tau_a(\omega)$ is shown in the inset of Fig. 4(a), and in the normal state shows a monotonic increase with frequency, and an overall downward shift with decreasing temperature. Below T_c , there is a strong suppression of $1/\tau_a(\omega)$ at low frequency associated with the formation of the superconducting gap, with a slight overshoot and then the recovery of the normal-state value at high

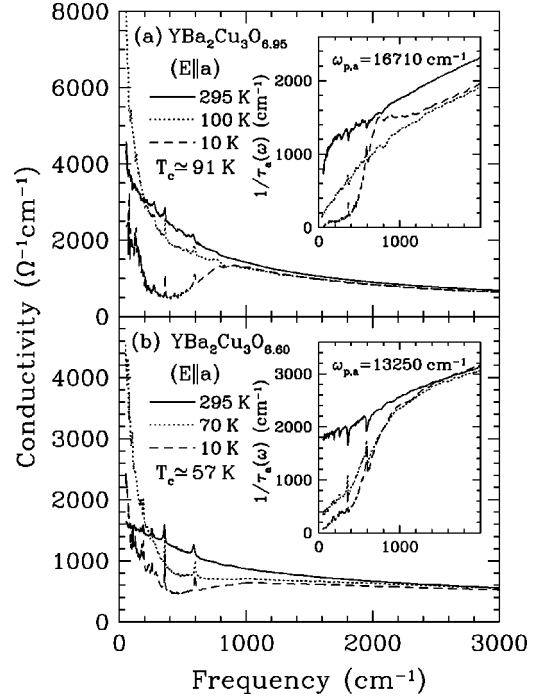


FIG. 4. The optical conductivity of (a) optimally doped $\text{YBa}_2\text{Cu}_3\text{O}_{6.95}$ and (b) underdoped $\text{YBa}_2\text{Cu}_3\text{O}_{6.60}$ at room temperature (solid line), $T \geq T_c$ (dotted line), and $T \leq T_c$ (dashed line) for light polarized along the a axis. The inset in each panel shows the frequency dependent scattering rate and the estimated value of $\omega_{p,a}$. The Drude-like conductivity of the optimally doped material narrows somewhat in the normal state but the scattering rate shows no indication of a pseudogap; below T_c a considerable amount of spectral weight collapses into the condensate. In the underdoped material, the conductivity narrows considerably in the normal state and the scattering rate indicates the opening of a pseudogap; the condensation is less dramatic than in the optimally doped case.

frequency.^{37,38} This behavior is characteristic of optimally doped and overdoped materials.

The behavior of the oxygen-underdoped material $\text{YBa}_2\text{Cu}_3\text{O}_{6.60}$ ($T_c \approx 57$ K) for light polarized along the a axis, shown in Fig. 4(b), shows some significant differences from the optimally doped material. The Drude-like conductivity at room temperature is extremely broad. However, at $T \approx T_c$ the Drude-like conductivity has narrowed dramatically, and there has been a significant shift of spectral weight to low frequencies. For $T \leq T_c$ the low frequency conductivity has decreased, indicating the formation of a condensate. However, the effect is not as dramatic as it was in the optimally doped material, indicating that the strength of the condensate is not as great. Once again, there is a considerable amount of residual conductivity at low frequency for $T \leq T_c$. The frequency-dependent scattering rate is shown in the inset, along with the estimated value of $\omega_{p,a} \approx 13250$ cm^{-1} , estimated from the conductivity sum rule. As the temperature decreases in the normal state $1/\tau_a(\omega)$ decreases rapidly at low frequency, which is taken to be evidence for the formation of a pseudogap.^{18,36} The large drop in the normal-state scattering rate for $1/\tau_a(\omega \rightarrow 0)$ is a reflection of the dramatic narrowing of the conductivity and is an

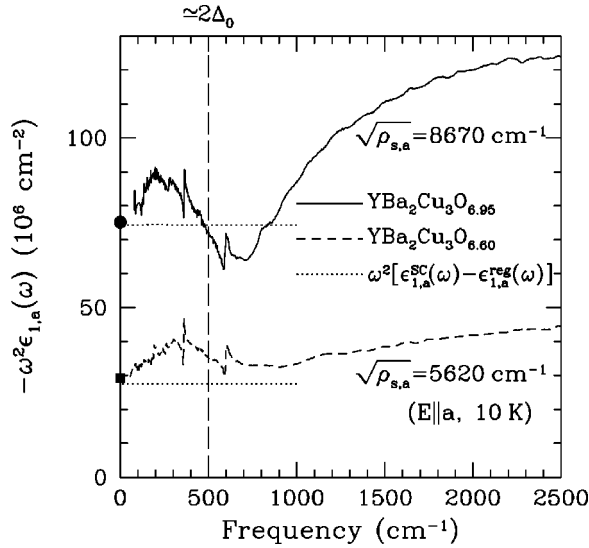


FIG. 5. The function $-\omega^2 \epsilon_{1,a}(\omega)$ vs frequency for optimally doped $\text{YBa}_2\text{Cu}_3\text{O}_{6.95}$ (solid line) and underdoped $\text{YBa}_2\text{Cu}_3\text{O}_{6.60}$ (dashed line) along the a axis at ≈ 10 K ($T \ll T_c$). The superfluid density is $\rho_s = -\omega^2 \epsilon_{1,a}(\omega \rightarrow 0)$; taking the squares to render the units the same as those of a plasma frequency yields $\sqrt{\rho_{s,a}} = 8670 \pm 90$ cm^{-1} and $\sqrt{\rho_{s,a}} = 5620 \pm 60$ cm^{-1} for the optimally and underdoped materials, respectively. Note also that in both materials there is a slight suppression of $-\omega^2 \epsilon_{1,a}(\omega)$ in the 500–700 cm^{-1} region, close to the estimated value of $2\Delta_0$.

indication that the reduced doping has not created a large amount of scattering due to disorder—on this basis, the system is *not* in the dirty limit.

The superfluid density $\rho_{s,a}$ has been estimated from the response of $-\omega^2 \epsilon_{1,a}(\omega)$ in the zero-frequency limit for $T \ll T_c$ for the optimally and underdoped materials, shown in Fig. 5. The estimate of $\rho_{s,a}$ assumes that the response of $\epsilon_{1,a}(\omega)$ at low frequency is dominated by the condensate, but it has been shown that along the c axis, there is enough residual conductivity to affect $\epsilon_{1,c}(\omega)$ and thus the values of $\rho_{s,c}$, typically resulting in an overestimate of the strength of the condensate.^{39,40} The presence of residual conductivity for $T \ll T_c$ suggests that $\rho_{s,a}$ may be overestimated in this case as well. However, as we noted earlier, the real part of the conductivity in the superconducting state may be expressed as a regular part due to unpaired carriers, and a $\delta(\omega)$ function at zero frequency; the response of $\epsilon_{2,a}^{SC}(\omega)$ is limited to the $\delta(\omega)$ function, which is zero elsewhere. However, $\epsilon_{2,a}(\omega)$ has been determined experimentally to be nonzero: if we refer to this as $\epsilon_{2,a}^{\text{reg}}(\omega)$, then $\epsilon_{1,a}^{\text{reg}}(\omega)$ may be determined through the Kramers-Kronig relation, and the superfluid density estimated as⁴⁰

$$\rho_{s,a}(\omega) = \omega^2 [\epsilon_{1,a}^{SC}(\omega) - \epsilon_{1,a}^{\text{reg}}(\omega)], \quad (6)$$

which should be a constant. This is shown in Fig. 5 at low frequency as the dotted lines. This method of estimating $\rho_{s,a}$ agrees well with the extrapolated values of $-\omega^2 \epsilon_1(\omega)$ in the $\omega \rightarrow 0$ limit, and indicates that if there is a correction to $\rho_{s,a}$ associated with the residual conductivity for $T \ll T_c$, then it is quite small. The estimated values for the condensate are

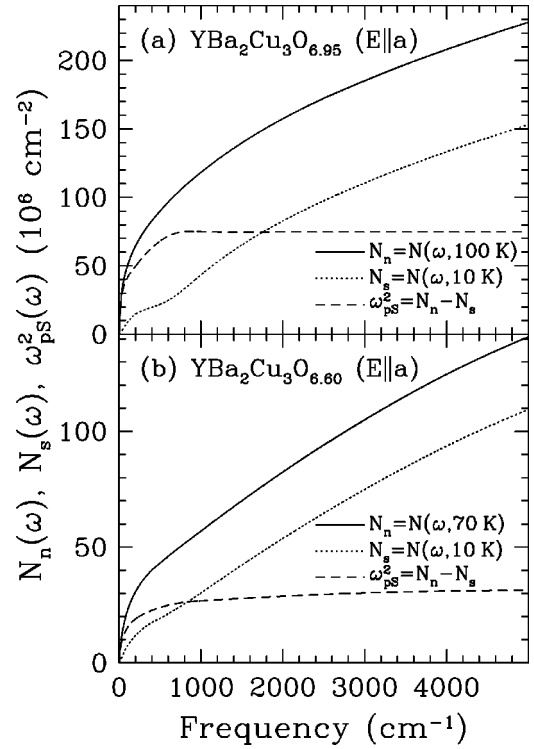


FIG. 6. The conductivity sum rules applied to (a) optimally doped $\text{YBa}_2\text{Cu}_3\text{O}_{6.95}$ and (b) underdoped $\text{YBa}_2\text{Cu}_3\text{O}_{6.60}$ for light polarized along the a axis for $T \geq T_c$ [$N_n(\omega)$, solid line] and for $T \ll T_c$ [$N_s(\omega)$, dotted line]; the difference is the estimate of the strength of the condensate from the Ferrell-Glover-Tinkham sum rule (dashed line). The condensate saturates in the upper panel by ≈ 800 cm^{-1} , while in the lower panel the frequency at which the full weight of the condensate is recovered seems to be much higher. In the upper panel the magnitudes of the curves are greater than in the lower panel; a reflection of the decreased carrier concentration.

$\sqrt{\rho_{s,a}} = 8670 \pm 90$ and 5620 ± 60 cm^{-1} for the optimally and underdoped materials, respectively; these estimates are in good agreement with previous values.³⁰ In both materials there is a slight suppression of $-\omega^2 \epsilon_1(\omega)$ in the 500–700 cm^{-1} region, which is in agreement with estimates for the superconducting gap maximum $2\Delta_0 \approx 500$ cm^{-1} (adopting the notation for a d -wave superconductor) in overdoped $\text{YBa}_2\text{Cu}_3\text{O}_{6.99}$ (Ref. 41). Studies of other cuprate systems suggest that the gap maximum increases with decreasing doping,^{12,42,43} despite the reduction of T_c .

The integrated values of the conductivity in the normal ($T \geq T_c$) and superconducting ($T \ll T_c$) states are indicated by the solid [$N_n(\omega)$] and dashed [$N_s(\omega)$] lines for $\text{YBa}_2\text{Cu}_3\text{O}_{6.95}$ and $\text{YBa}_2\text{Cu}_3\text{O}_{6.60}$ along the a axis in the upper and lower panels of Fig. 6, respectively. For $\text{YBa}_2\text{Cu}_3\text{O}_{6.95}$, $N_n(\omega)$ increases rapidly with frequency, but does not display any unusual structure. On the other hand, $N_s(\omega)$ evolves more slowly, and has several inflection points at low frequency which are thought to be related to the peaks in the electron-boson spectral function.⁴⁴ The difference between the two curves $\omega_{pS}^2 = N_n(\omega) - N_s(\omega)$ is shown by the dashed line in Fig. 6(a). This quantity increases quickly and then saturates above ≈ 800 cm^{-1} to a constant value. this

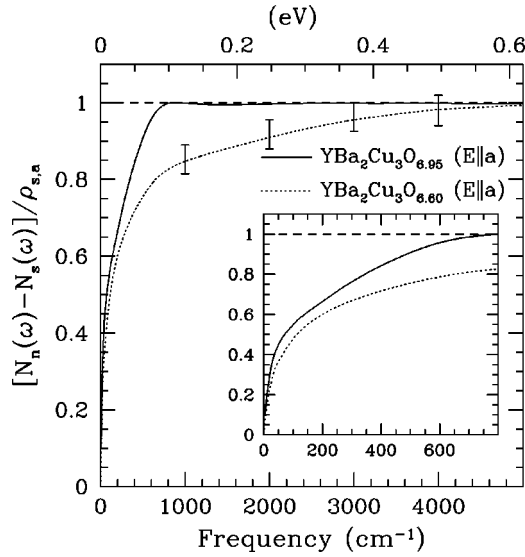


FIG. 7. The normalized weight of the condensate $[N_n(\omega) - N_s(\omega)]/\rho_{s,a}$ for optimally doped $\text{YBa}_2\text{Cu}_3\text{O}_{6.95}$ (solid line) and underdoped $\text{YBa}_2\text{Cu}_3\text{O}_{6.60}$ (dotted line) along the a axis direction. The curves describing the condensate have been normalized to the values of $\rho_{s,a}$ shown in Fig. 5. The condensate for the optimally doped material has saturated by $\approx 800 \text{ cm}^{-1}$, while in the underdoped material the condensate is roughly 80% formed by this frequency, but the other 20% is not recovered until much higher frequencies. The error bars on the curve for the underdoped material indicate the uncertainty associated with the FGT sum rule. Inset: The low-frequency region.

plot is reminiscent of the BCS material with moderate scattering, discussed in Fig. 3(b). The sum rules applied to $\text{YBa}_2\text{Cu}_3\text{O}_{6.60}$ shown in Fig. 6(b) are similar to the optimally doped case. However, the overall magnitude has decreased, a reflection of the decreased carrier concentration within the copper-oxygen planes in the underdoped material. While the condensate is also lower, it now appears that it does not saturate as quickly as was the case in the optimally doped material.

A more detailed examination of the evolution of the weight of the condensate for $\text{YBa}_2\text{Cu}_3\text{O}_{6.95}$ (solid line) and $\text{YBa}_2\text{Cu}_3\text{O}_{6.60}$ (dotted line), normalized to the values of $\rho_{s,a}$ determined in Fig. 5, is shown in Fig. 7. The error associated with the FGT sum rule has been determined in the following way. The optical conductivity has been calculated for $R(\omega, T) \pm 0.1\%$ for $T \geq T_c$ and $T \leq T_c$, the normal and superconducting states, respectively. The FGT sum rule is then applied to the resulting high and low values for the conductivity, and the error limits are taken as the deviation from the curve generated simply from $R(\omega, T)$, which are estimated to be about $\pm 3\%$. It should be noted that most of the uncertainty is introduced when the reflectance is close to unity, as $\sigma_1 \propto 1/(1-R)$ and even small uncertainties in the reflectance can lead to large errors in the optical conductivity. When the FGT sum rule is exhausted, the ratio is unity by definition. For the optimally doped material, this occurs rapidly and 90% of the spectral weight in the has been recovered by about 500 cm^{-1} , and the ratio approaches unity at $\omega_c \approx 800 \text{ cm}^{-1}$, and remains constant even out to very high

frequencies (over 0.5 eV). This rapid formation of the condensate has also been observed in the optimally doped materials^{45,46} $\text{La}_{1.85}\text{Sr}_{0.15}\text{CuO}_4$ ($\omega_c \approx 0.05 \text{ eV}$), $\text{Bi}_2\text{Sr}_2\text{CaCu}_2\text{O}_{8+\delta}$ ($\omega_c \approx 0.1 \text{ eV}$), as well as in the electron-doped material $\text{Nd}_{1.85}\text{Ce}_{0.15}\text{CuO}_{4+\delta}$ ($\omega_c \approx 0.06 \text{ eV}$). In all of these cases the integral saturates and is constant to over 0.5 eV. In contrast, only about 80% the spectral weight in underdoped $\text{YBa}_2\text{Cu}_3\text{O}_{6.60}$ has formed by 800 cm^{-1} ; the 90% threshold is not reached until $\approx 1800 \text{ cm}^{-1}$ and the remaining spectral weight is recovered only at much higher frequencies ($\omega_c \geq 5000 \text{ cm}^{-1}$). In the case of the underdoped material, the plot has only been shown to the point where the FGT sum rule is recovered. If the plot is extended to $\sim 1 \text{ eV}$, then the integral will increase to a value about $\approx 3\%$ over unity, which is within the estimated error for the FGT sum rule. This slow increase above unity may be an indication of one of two things: (i) ω_c may be larger than has been previously estimated, which would be consistent with estimates of $\omega_c \approx 2 \text{ eV}$ in the underdoped $\text{Bi}_2\text{Sr}_2\text{CaCu}_2\text{O}_{8+\delta}$ materials²³ or (ii) it is possible that when the sum rule is extended to high frequencies (i.e., of the order of eV) it may be incorporating temperature-dependent bound excitations. However, the absence of this behavior in the optimally doped system suggests that such an excitation is restricted to the underdoped materials.

It is tempting to draw an analogy with the BCS dirty-limit case and argue that the spectral weight in the underdoped material has been pushed to higher frequency in response to an increase in the normal-state scattering rate. However, there are two important points that argue against this interpretation. First, an examination of scattering rate in the insets of Fig. 4 for $T \geq T_c$ indicates that the $1/\tau_a(\omega \rightarrow 0) \leq 200 \text{ cm}^{-1}$ for both materials. Second, if the conductivity is fitted using a two-component Drude-Lorentz model, then the nature of the low-frequency conductivity places hard constraints on the width of the Drude peak;⁴⁸ for $T \geq T_c$ then $\Gamma \approx 140 \text{ cm}^{-1}$ for optimally doped $\text{YBa}_2\text{Cu}_3\text{O}_{6.95}$, and $\Gamma \approx 100 \text{ cm}^{-1}$ for underdoped $\text{YBa}_2\text{Cu}_3\text{O}_{6.60}$. In each case, $\Gamma < 2\Delta_0$, indicating that while Γ may have an unusual temperature dependence, close to T_c these materials are not in the dirty limit. Thus, the larger energy scale in the underdoped system has a different origin. While none of the cuprate superconductors are truly good metals, it has been suggested that for $T \geq T_c$ the overdoped materials may resemble a Fermi liquid.⁴⁹ The rapid convergence of $\rho_{s,a}$ in the optimally doped material is what would be expected in a BCS system in which the normal state is a Fermi liquid. On the other hand, it is recognized that the underdoped materials are bad metals⁵⁰ and exhibit non-Fermi-liquid behavior, and $\omega_c \gg 2\Delta_0$ is required to recover the FGT sum rule. The two types of behavior observed in the optimal and underdoped materials suggests that the nature of the electronic correlations in the normal state play a role in determining the different aspects of the superconductivity observed in these materials.^{19,51}

C. Kinetic energy and the sum rule

The unconventional nature of the superconductivity in the cuprate systems has led to the suggestion that the conden-

sation may be driven by changes in the kinetic rather than the potential energy.⁶ In such a case the FGT sum rule for the in-plane conductivity must be modified to take on the form⁷

$$\begin{aligned} \rho_s &= \frac{120}{\pi} \int_{0+}^{\omega_c} [\sigma_{1,n}(\omega) - \sigma_{1,s}(\omega)] d\omega \\ &+ \frac{e^2 a^2}{\pi c^2 \hbar^2} [\langle -T_s \rangle - \langle -T_n \rangle], \\ &\equiv \delta A_l + \delta A_h, \end{aligned} \quad (7)$$

where the spectral weight has units of cm^{-2} , a is the lattice spacing, T is that part of the in-plane kinetic energy associated with the valence band,^{7,8} and the subscripts n and s refer to $T \approx T_c$ and $T \ll T_c$, respectively. (The expression has a slightly different form for the c axis.⁵²⁻⁵⁴) The low-frequency term δA_l is simply the FGT sum rule, while δA_h corresponds to the high-frequency part of the integral, which is in fact the kinetic energy contribution. In a system where the kinetic energy plays a prominent role the FGT sum rule may appear to be violated. However, the maximum condensation energy for $\text{YBa}_2\text{Cu}_3\text{O}_{6.95}$ based on specific heat measurements^{55,56} is about 0.2 meV per (in-plane) copper atom. Assuming that the condensation energy is due entirely to the changes in the in-plane kinetic energy, this yields $\delta A_h \approx 2 \times 10^5 \text{ cm}^{-2}$, which represents less than 0.3% of the spectral weight of the condensate.⁵⁷ Because of the limited accuracy of the FGT sum rule no statement may be made regarding changes in the in-plane kinetic energy. However, the general observation that the in-plane sum rule is preserved may have consequences for the c axis.

D. Sum rules along the c axis

The optical properties of $\text{YBa}_2\text{Cu}_3\text{O}_{6+x}$ have been examined in some detail along the poorly conducting c axis.⁵⁸⁻⁶¹ The optical conductivity (especially in the underdoped materials) is dominated by the unscreened phonons.^{62,63} Given that large changes in the phonon spectrum have been observed at low temperature in the underdoped materials,⁶²⁻⁶⁶ the application of the FGT sum rule must be treated with some care; in the studies cited here,^{16,17} the integral has been truncated at $\omega_c \approx 800 \text{ cm}^{-1}$ (0.1 eV). The application of the FGT sum rule along the c axis has shown that while this sum rule is not violated in the optimally doped materials, as these materials become increasingly underdoped and a pseudogap has formed, the FGT sum rule is violated to varying degrees, with more than 50% of the c -axis spectral weight is missing at low temperature.^{16,17} The violation of the FGT sum rule has been proposed as evidence for a kinetic energy contribution,^{52,53} although there have also been other inter-

pretations of this phenomena.^{54,67} The implication is that the missing spectral weight is recovered at high frequency, but it is unclear at precisely what point this occurs. In underdoped material, if the value for $\omega_c = 800 \text{ cm}^{-1}$ in the optimally doped materials is used, then the in-plane FGT sum rule will appear to be violated. However, it has been shown that extending the integral from $\omega_c \approx 800$ to $\approx 5000 \text{ cm}^{-1}$ results in the recovery of the in-plane sum rule. We speculate that if the cutoff frequency for the FGT sum rule along the c axis is increased to the same value where the in-plane sum rule was recovered ($\omega_c \geq 5000 \text{ cm}^{-1}$) then the spectral weight would be recovered and the c axis sum rule would yield $\rho_{s,c}$. However, the general consensus at this time is that the conductivity data is not yet sufficiently precise along the c axis to confirm this prediction, so this remains a subject of some debate.

IV. CONCLUSIONS

In the BCS model the relevant energy scale to recover the strength of the condensate ρ_s is the superconducting energy gap ($\omega_c \approx 2\Delta$), slightly larger in the dirty-limit case. Conductivity and FGT sum rules have been examined for light polarized along the a axis direction in the optimally doped $\text{YBa}_2\text{Cu}_3\text{O}_{6.95}$ and underdoped $\text{YBa}_2\text{Cu}_3\text{O}_{6.60}$ high-temperature superconductors to study the evolution of the spectral weight in these materials. Within the sensitivity of the experiment the FGT sum rule is obeyed in both materials. The energy scale required to recover the full strength of the condensate in the optimally doped material is $\omega_c \approx 800 \text{ cm}^{-1}$ ($\approx 2\Delta_0$), in good agreement with the predicted behavior of the BCS model. However, the energy scale in the underdoped materials is much higher, $\omega_c \geq 5000 \text{ cm}^{-1}$. This effect cannot be attributed to dirty-limit effects in response to increased normal-state scattering, since for $T \approx T_c$, $\Gamma < 2\Delta_0$ in both materials. The two types of behavior above and below T_c observed in the optimal and underdoped materials suggests that the nature of the electronic correlations in the normal state determine the different aspects superconductivity in these materials,¹⁹ and the degree to which the kinetic energy may play a role.

ACKNOWLEDGMENTS

We are grateful to D. van der Marel for insights regarding the specific heat results. We would also like to thank D. N. Basov, V. J. Emery, A. Chubukov, S. A. Kivelson, F. Margiglio, C. Pépin, M. Strongin, D. B. Tanner, T. Timusk, J. M. Tranquada, and J. J. Tu for useful discussions. This work was supported by the Department of Energy under Contract No. DE-AC02-98CH10886 and by the Canadian Institute for Advanced Research.

*Electronic address: homes@bnl.gov

¹D.Y. Smith, in *Handbook of Optical Constants of Solids*, edited by E.D. Palik (Academic, New York, 1985), pp. 35-68.

²R.A. Ferrell and R.E. Glover III, *Phys. Rev.* **109**, 1398 (1958).

³M. Tinkham and R.A. Ferrell, *Phys. Rev. Lett.* **2**, 331 (1959).

⁴J. Bardeen, L.N. Cooper, and J.R. Schrieffer, *Phys. Rev.* **108**, 1175 (1957).

⁵M. Tinkham, *Introduction to Superconductivity* (McGraw-Hill, New York, 1966).

⁶J. Hirsch, *Physica C* **199**, 305 (1992).

- ⁷J.E. Hirsch and F. Marsiglio, Phys. Rev. B **62**, 15 131 (2000).
- ⁸J.E. Hirsch and F. Marsiglio, Physica C **331**, 150 (2000).
- ⁹M.R. Norman, M. Randeria, B. Jankó, and J.C. Campuzano, Phys. Rev. B **61**, 14 742 (2000).
- ¹⁰R. Haslinger and A.V. Chubukov, Phys. Rev. B **67**, 140504 (2003).
- ¹¹P.A. Lee, Physica C **317**, 194 (1999).
- ¹²P.W. Anderson, Physica C **341-348**, 9 (2000).
- ¹³V.J. Emery and S.A. Kivelson, J. Phys. Chem. Solids **61**, 467 (2000).
- ¹⁴S. Alexandrov and N.F. Mott, *High Temperature Superconductors and Other Superfluids* (Taylor and Francis, London, 1994).
- ¹⁵M.V. Klein and G. Blumberg, Science **283**, 42 (1999).
- ¹⁶D.N. Basov, S.I. Woods, A.S. Katz, E.J. Singley, R.C. Dynes, M. Xu, D.G. Hinks, C.C. Homes, and M. Strongin, Science **283**, 49 (1999).
- ¹⁷D.N. Basov, C.C. Homes, E.J. Singley, M. Strongin, T. Timusk, G. Blumberg, and D. van der Marel, Phys. Rev. B **63**, 134514 (2001).
- ¹⁸T. Timusk and B. Statt, Rep. Prog. Phys. **62**, 61 (1999).
- ¹⁹M.R. Norman and C. Pépin, Phys. Rev. B **66**, 100506 (2002).
- ²⁰D. van der Marel (private communication).
- ²¹H.J.A. Molegraaf, C. Presura, D. van der Marel, P.H. Kes, and M. Li, Science **295**, 2239 (2002).
- ²²A.F. Santander-Syro, R.P.S.M. Lobo, N. Bontemps, Z. Konstantinovic, Z. Li, and H. Raffy, Phys. Rev. Lett. **88**, 097005 (2002).
- ²³A.F. Santander-Syro, R.P.S.M. Lobo, N. Bontemps, Z. Konstantinovic, Z.Z. Li, and H. Raffy, Europhys. Lett. **62**, 568 (2003).
- ²⁴R. Liang, P. Dosanjh, D.A. Bonn, D.J. Baar, J.F. Carolan, and W.N. Hardy, Physica C **195**, 51 (1992).
- ²⁵P. Schleger, W.N. Hardy, and B.X. Yang, Physica C **176**, 261 (1991).
- ²⁶C.C. Homes, M. Reedyk, D. Cradles, and T. Timusk, Appl. Opt. **32**, 2976 (1993).
- ²⁷D.N. Basov, R. Liang, D.A. Bonn, W.N. Hardy, B. Dabrowski, M. Quijada, D.B. Tanner, J.P. Rice, D.M. Ginsberg, and T. Timusk, Phys. Rev. Lett. **74**, 598 (1995).
- ²⁸D.N. Basov, R. Liang, B. Dabrowski, D.A. Bonn, W.N. Hardy, and T. Timusk, Phys. Rev. Lett. **77**, 4090 (1996).
- ²⁹H. Romberg, N. Nücker, J. Fink, T. Wolf, X.X. Xi, B. Koch, H.P. Geserich, M. Dürer, W. Assmus, and B. Gegenheimer, Z. Phys. B: Condens. Matter **78**, 367 (1990).
- ³⁰C.C. Homes, D.A. Bonn, R. Liang, W.N. Hardy, D.N. Basov, T. Timusk, and B.P. Clayman, Phys. Rev. B **60**, 9782 (1999).
- ³¹The term $120/\pi$ before the integral assumes that the units of conductivity are in $\Omega^{-1}\text{cm}^{-1}$, and that the frequency is in cm^{-1} , so that the integral yields cm^{-2} . The factor in front of the integral is sometimes expressed as $2m^*V_c/\pi e^2$, where V_c is the volume of the unit cell, in which case the integral yields the effective number of carriers.
- ³²V.J. Emery and S.A. Kivelson, Nature (London) **374**, 343 (1995).
- ³³W. Zimmerman, E.H. Brandt, M. Bauer, E. Seider, and L. Genzel, Physica C **183**, 99 (1991).
- ³⁴D.B. Tanner and T. Timusk, in *Physical Properties of High Temperature Superconductors III*, edited by D.M. Ginsberg (World Scientific, Singapore, 1992), p. 408.
- ³⁵B.C. Webb, A.J. Sievers, and T. Mihalisin, Phys. Rev. Lett. **57**, 1951 (1986).
- ³⁶A.V. Puchkov, D.N. Basov, and T. Timusk, J. Phys.: Condens. Matter **8**, 10 049 (1996).
- ³⁷D.N. Basov, E.J. Singley, and S.V. Dordevic, Phys. Rev. B **65**, 054516 (2002).
- ³⁸A. Abanov and A.V. Chubukov, Phys. Rev. Lett. **88**, 217001 (2002).
- ³⁹C.C. Homes, S. Kamal, D.A. Bonn, R. Liang, W.N. Hardy, and B.P. Clayman, Physica C **296**, 230 (1998).
- ⁴⁰S.V. Dordevic, E.J. Singley, D.N. Basov, S. Komiyama, Y. Ando, E. Bucher, C.C. Homes, and M. Strongin, Phys. Rev. B **65**, 134511 (2002).
- ⁴¹D.H. Lu, D.L. Feng, N.P. Armitage, K.M. Shen, A. Damascelli, C. Kim, F. Ronning, Z.-X. Shen, D.A. Bonn, R. Liang, W.N. Hardy, A.I. Rykov, and S. Tajima, Phys. Rev. Lett. **86**, 4370 (2001).
- ⁴²J.M. Harris, Z.-X. Shen, P.J. White, D.S. Marshall, M.C. Schabel, J.N. Eckstein, and I. Bozovic, Phys. Rev. B **54**, R15 665 (1996).
- ⁴³N. Miyakawa, J.F. Zasadzinski, L. Ozyuzer, P. Guptasarma, D.G. Hinks, C. Kendziora, and K.E. Gray, Phys. Rev. Lett. **83**, 1018 (1999).
- ⁴⁴J.J. Tu, C.C. Homes, G.D. Gu, D.N. Basov, and M. Strongin, Phys. Rev. B **66**, 144514 (2002).
- ⁴⁵D.B. Tanner, H.L. Liu, M.A. Quijada, A.M. Zibold, H. Berger, R.J. Kelley, M. Onellion, F.C. Chou, D.C. Johnston, J.P. Rice, D.M. Ginsberg, and J.T. Markert, Physica B **244**, 1 (1998).
- ⁴⁶J.J. Tu (private communication).
- ⁴⁷C.C. Homes, B.P. Clayman, J.L. Peng, and R.L. Greene, Phys. Rev. B **56**, 5525 (1997).
- ⁴⁸M.A. Quijada, D.B. Tanner, R.J. Kelley, M. Onellion, H. Berger, and G. Margaritondo, Phys. Rev. B **60**, 14 917 (1999).
- ⁴⁹C. Proust, E. Boaknin, R.W. Hill, L. Taillefer, and A.P. Mackenzie, Phys. Rev. Lett. **89**, 147003 (2002).
- ⁵⁰V.J. Emery and S.A. Kivelson, Phys. Rev. Lett. **74**, 3253 (1995).
- ⁵¹A. Iyengar, J. Stajic, Y.-J. Kao, and K. Levin, Phys. Rev. Lett. **90**, 187003 (2003).
- ⁵²S. Chakravarty, Eur. Phys. J. B **5**, 337 (1998).
- ⁵³S. Chakravarty, H.-Y. Kee, and E. Abrahams, Phys. Rev. Lett. **82**, 2366 (1999).
- ⁵⁴D. Munzar, C. Bernhard, T. Holden, A. Golnik, J. Humlíček, and M. Cardona, Phys. Rev. B **64**, 024523 (2001).
- ⁵⁵J.W. Loram, J. Luo, J.R. Cooper, W.Y. Liang, and J.L. Tallon, J. Phys. Chem. Solids **62**, 59 (2001).
- ⁵⁶D. van der Marel, A.J. Leggett, J.W. Loram, and J.R. Kirtely, Phys. Rev. B **66**, 140501 (2002).
- ⁵⁷The specific heat measurements of Loram *et al.* [J. Phys. Chem. Solids **62**, 59 (2001), see Fig. 9] for $\text{Y}_{0.8}\text{Ca}_{0.2}\text{Ba}_2\text{Cu}_3\text{O}_{6+x}$ (taken as optimally doped) yield a maximum condensation energy of $U(0) \approx 3\text{J}/(\text{g at.})$, or about $3.6 \times 10^6 \text{erg}/\text{cm}^3$ or 0.2 meV per in-plane copper atom. Allowing that the condensation energy $U(0)$ is entirely due to a change in the in-plane kinetic energy, then the contribution along the a -axis direction may be taken as $U(0)/2$. From the text, $\delta A_h = e^2 a^2 / \pi c^2 \hbar^2 [U(0)/2]$, taking $a \approx 3.8 \text{Å}$ as the lattice constant, then $\delta A_h \approx 1.9 \times 10^5 \text{cm}^{-2}$, which represents $\approx 0.25\%$ of the measured spectral weight of $\rho_{s,a} = 7.52 \times 10^7 \text{cm}^{-2}$ in $\text{YBa}_2\text{Cu}_3\text{O}_{6.95}$.
- ⁵⁸C.C. Homes, T. Timusk, D.A. Bonn, R. Liang, and W.N. Hardy, Phys. Rev. Lett. **71**, 1645 (1993).
- ⁵⁹J. Schützmann, S. Tajima, S. Miyamoto, and S. Tanaka, Phys.

- Rev. Lett. **73**, 174 (1994).
- ⁶⁰C.C. Homes, T. Timusk, D.A. Bonn, R. Liang, and W.N. Hardy, Physica C **254**, 265 (1995).
- ⁶¹S. Tajima, J. Schützmann, S. Miyamoto, I. Terasaki, Y. Sato, and R. Hauff, Phys. Rev. B **55**, 6051 (1997).
- ⁶²C.C. Homes, T. Timusk, D.A. Bonn, R. Liang, and W.N. Hardy, Can. J. Phys. **73**, 663 (1995).
- ⁶³J. Schützmann, S. Tajima, S. Miyamoto, Y. Sato, and R. Hauff, Phys. Rev. B **52**, 13 665 (1995).
- ⁶⁴D. Munzar, C. Bernhard, A. Golnik, J. Humlíček, and M. Cardona, Solid State Commun. **112**, 365 (1999).
- ⁶⁵M. Grüninger, D. van der Marel, A.A. Tsvetkov, and A. Erb, Phys. Rev. Lett. **84**, 1575 (2000).
- ⁶⁶C. Bernhard, D. Munzar, A. Golnik, C.T. Lin, A. Wittlin, J. Humlíček, and M. Cardona, Phys. Rev. B **61**, 618 (2000).
- ⁶⁷L.B. Ioffe and A.J. Millis, Science **285**, 1241 (1999).